Interval Type-2 fuzzy set and theory of weak continuity constraints for accurate multi-class image segmentation

Soumyadip Dhar*, Malay K Kundu†, *Senior Member, IEEE*
*RCC Institute of Information Technology,Kolkata-700015,India, rccsoumya@gmail.com
†Indian Statistical Institute,Kolkata-700108,India, malay@isical.ac.in

***Abstract*—Multi-class image segmentation is a challenging task due to the uncertainties involved with the process of segmentation. To handle those uncertainties, we propose an automatic multi-class image segmentation method based on an interval type-2 fuzzy set(IT2FS). In the proposed method, the accurate multi-class segmentation is achieved by minimizing an energy function. This energy function is based on IT2FS and weak continuity constraints present in the membership values. The theory of weak continuity constraints helps to localize the segmentation boundaries between the classes accurately with the minimization of the energy. The proper localization of segmentation boundaries helps to minimize the uncertainties in the segmentation process. We also theoretically show that the minimization of the energy function reduces the uncertainties present in the segmentation process. Furthermore, the method automatically determines the number of clusters without a priori knowledge. The proposed method is found to be superior to the existing conventional, fuzzy type-1 and fuzzy type-2 based segmentation techniques. The superiority is verified using synthetic and benchmark datasets. The noise immunity of the proposed method is found to be better than that of the state-of-the-art methods when benchmark against the modified Cramer-Rao bound.**

***Index Terms*—Type-2 fuzzy set, weak continuity constraints, COG, image segmentation, thresholding**

I. INTRODUCTION

Image multi-thresholding is one of the basic and useful techniques for multi-class image segmentation. The objective of multi-class image segmentation is to group the pixels based on the image properties like pixel value, color, and texture of the image. The group would be such that the intra-class variation of the pixels becomes as low as possible. Not only this, an efficient segmentation process must mark the boundaries between the different segments clearly. The determination of segmentation boundaries between different class regions is an ill-posed problem. This is due to the uncertainty involved in simultaneous detection of intensity change and corresponding position with equal accuracy[1]. Another challenge is to determine the correct number of segments in an image automatically without a prior knowledge. The segmentation using thresholding process has a wide variety of real-life applications[2], [3]. They include metal industries, agriculture industries, and medical science.

In the literature, several strategies for multi-class image segmentation are found. They can be classified into two categories; one is parametric[4]–[6] and another is non-parametric [7]–[17]. The statistical distribution of each class is pre-assumed for segmentation in a parametric method. On the other hand, a non-parametric method is the parameter-free approach and are widely used for image segmentation[13]. Apart from these broad categories, image segmentation can be done by different methods like region based methods[18]–[20], Graph-based image segmentation[21]–[23], edge-based method[24], [25] and thresholding based methods[26]–[28]. The conventional approaches mentioned above are unable to minimize the uncertainties in image segmentation. Thus, they are not efficient for simultaneous localization and detection of segmentation boundaries.

In order to develop a robust segmentation process, which is capable of handling uncertainties involved in simultaneous localization and detection of segmentation boundaries, we need a proper tool. The tool should reduce the gray level and spatial ambiguity in an image to reduce the uncertainties. Moreover, if possible, a suitable guideline need to develop in order to decide the correct number of segmentation classes/clusters without any prior knowledge.

A number of methods can be found in the literature which can handle the uncertainties in the image segmentation. Most of the methods[29]–[31] used the fuzzy set theory introduced by Zadeh[32] as an uncertainty handling tool. Most of the cases it is customary to use the type-1 fuzzy set for uncertainty handling. However, in a few special cases where (1) data are not clean(noise free) (2) hazy or (3) partial, the type-1 fuzzy set based system could not able to produce results to the full satisfaction of the user. In this case, IT2FS can produce much better results[33] although it is computationally costly than type-1 fuzzy set. So, some researches used type-2 set for image segmentation. The type-2 fuzzy set has better uncertainty handling capacity as their membership functions are fuzzy, not crisp. As a result, it possesses additional degrees of freedom. The additional degrees of freedom helps to model the uncertainties accurately. It could handle the uncertainties due to different types of perturbations in an image[34]. Again, due to the simple nature of membership functions, the interval type-2 fuzzy set (IT2FS) is quite popular for practical applications[35]. Type-2 fuzzy c-means based image segmentations were proposed by [36]–[39]. Again, the methods in [40]–[42] presented the thresholding based approach for image segmentation in the type-2 fuzzy domain.

In fuzzy based image segmentation the input image is

converted into the fuzzy set by indicating the degree of belongingness of each pixel in different segments. Though the fuzzy set is a powerful tool for handling uncertainties, mapping into crisp pixel domain is required at the end to facilitate the interpretation of the segments. In IT2FS the segmentation is achieved either by minimizing the global fuzzy entropy(based on intervals)[40], [41], [43] or by minimizing an objective function which is the weighted average of the pixel distances from the cluster center[44]. This is followed by a process where the fuzzy set is replaced by a crisp set by the method of defuzzification. But, both the methods could not achieve the highest level of accuracy. This is due to the fact these approaches use only the global information and ignore the local information for detection of segmentation boundaries and they may bias towards high/low membership values. In fact, the other existing uncertainty measures of the IT2FS also do not consider the neighborhood information of a data[45]. Again, both the type-1 and type-2 based approach assume some arbitrary knowledge about the number of segmentation classes.

In order to overcome both of the above-mentioned problems for getting better multi-class boundaries, we propose a novel iterative multi-class image segmentation method based on the IT2FS. Here, by the term 'class' we denote the meaningful regions or segments but not the labeling of the segments. In this method, we use the IT2FS as an uncertainty handling tool with a modified technique to determine the accurate segmentation boundaries. The method incorporates both the global and local statistics of the image in hand and reduces the uncertainties in the segmentation. In order to completely locate the true segmentation boundaries, a technique called weak continuity constraints is incorporated.

Weak continuity constraints were used successfully for visual reconstruction of discrete data[46], [47]. According to [46]- *'The power of weak continuity constraints lies in their ability to detect discontinuities and localize them accurately and robustly. Conventional methods for finding discontinuities would blur the signal then look for the feature points such as point of steepest gradients. The weak string, however, preserves discontinuities without any prior information about the existence or location.'*. Segmentation boundaries may not be strong due to the low-intensity variation between the classes. A global ad-hoc thresholding disconnects the weak (low value of the gradient) boundaries. The weak continuity constraints property localizes the boundaries even in low gradient or in presence of substantial noise. Thus, the thresholding with the help of weak continuity constraints helps to reduce the ambiguities in the image, which in turn minimize the uncertainties prevailing in the segmentation process.

The novelties of the proposed method are: (1) Here we fit the pixels of the image into different segments by an IT2FS based energy function. For creating the energy function, we adopt the theory of weak string under weak continuity constraints[46]. According to the theory, the string tries to become stable by residing in the lowest energy. At the point of weak continuity, the string snaps due to the violation of weak continuity constraints and discontinuity are localized. In the segmentation, the segmentation boundaries are the points of discontinuity between the segments which violates the weak continuity constraints. The accurate segments are obtained by minimizing the energy function which acts as an objective function for the image segmentation. Minimization of the energy function reduces the gray level and spatial ambiguities in an image. The reduction of the ambiguities helps to localize the segmentation boundaries accurately with the reduction of the uncertainties in the segmentation process. (2) We theoretically prove that the minimization of the energy reduces the uncertainties. (3) Another contribution of the paper is that here we propose the IT2FS based criteria for automatic generation of image segments without a priori knowledge. We also prove that it is the general method from which the popular and benchmark Otsu technique can be derived.

The rest of the paper is as follows. The theory of type-2 fuzzy set and mapping of an image into an IT2FS are discussed in Section II. Section III describes the weak continuity constraints and energy function for segmentation. The automatic generation of classes with an iterative scheme and the proposed algorithm are discussed in sectionIV. Section V and sectionVI describe the performance measure, experimental results, performance comparison, and limitation of the proposed method.

II. Mapping of image segments into interval type-2 fuzzy set

In the proposed method the image segments are mapped into IT2FS. In the followings subsections, we will discuss the IT2FS briefly and the mapping procedure.

1) Interval type-2 fuzzy set: In a type-2 fuzzy set(T2FS), the MF(membership function) is also fuzzy. A type-2 set $\widetilde{A}$ is specified by type-2 fuzzy membership(T2MF) function $\mu_{\widetilde{A}}(x,u)$, where $x \in X$,i.e

$$\widetilde{A} = \{((x,u), \mu_{\widetilde{A}}(x,u)) | \forall x \in X, \forall u \in J_x \subseteq [0,1]\} \quad (1)$$

in which $0 \leq \mu_{\widetilde{A}}(x,u) \leq 1$. $\widetilde{A}$ can also be formulated as

$$\widetilde{A} = \int_{x \in X} \int_{u \in J_x} \mu_{\widetilde{A}}(x,u)/(x,u), J_x \subseteq [0,1] \quad (2)$$

where $\mu_{\widetilde{A}}(x,u)$ is the secondary membership function and J_x is the primary membership of x, and it is the secondary membership function domain. Here $\int\int$ denotes union over all permissible x and u. For discrete set $\int$ is given by $\sum$. When all $\mu_{\widetilde{A}}(x,u) = 1$ in the Eq.2 ,then $\widetilde{A}$ represents the interval type-2 fuzzy set(IT2FS)[48]. That means in IT2FMF, the secondary grade which is the amplitude of secondary MF becomes one.

A. Mapping of image segments into Interval type-2 Fuzzy set

In the proposed method, an image L level is fuzzified with respect to the threshold t. A pixel intensity below t is considered as an element of background(object) segment I_b and a pixel above t is considered as an element of object(background) segment I_o. Since t is the transition point or changing point from one segment to another, it can be used for localization of the boundary point. In the proposed method

the type-1 fuzzy membership function for the two segments of the image I is given by

$$\mu(x) = \begin{cases} 1 - \left(\frac{x}{t}\right)^{k3} & \text{if } x \leq t \\ 1 - \left(\frac{L-x}{L-t}\right)^{k4} & \text{if } x > t \end{cases} \quad (3)$$

where $k3, k4 > 0$.

To generate the IT2MF membership function from the above type-1 membership function we use the blurring technique[40]. In the blurring technique, the upper membership value $\overline{\mu}$ and the lower membership value $\underline{\mu}$ are given by

$$\overline{\mu}(x) = \mu(x)^{\frac{1}{\beta}}$$
$$\underline{\mu}(x) = \mu(x)^{\beta} \quad (4)$$

where $\beta \in (1, \infty)$. From the Eq 4 it is clear that the different fuzzy sets are produced for different values of t. In fuzzy theory, the proper fuzzy sets which can represent the different segments properly are achieved either by minimizing(or maximizing) fuzzy entropy or by minimizing an objective function which represents the fuzzy weighted average of the pixels from cluster(segment) center. Both the measures are global and biased towards high(low) interval or high membership values and unable to reduce the uncertainties prevailing in the localization of segmentation boundaries. To evade the problem, we model an energy function using weak continuity constraints in the membership values to generate the proper threshold values for creating the segments.

III. Interval type-2 fuzzy based segmentation using weak continuity constraints

A. Theory of weak continuity constraints

The weak continuity constraints represent the constraints which can only be violated with a cost. That means, some penalty is related to the localization of discontinuities. In the proposed technique, we adopt the weak elastic string energy concept[49] for implementation of weak continuity constraints. The purpose of weak elastic string in computer vision is to construct a piecewise linear function $u_{str}(x)$ to fit a discrete data $d_{str}(x)$ [49]. In this reconstruction process $u_{str}(x)$ behaves like a string and it is stable at low energy state. The string will be snapped with a penalty at the points where it violates the weak continuity constraints to attain the minimum energy. That means discontinuity will be detected at those points. The concept can be understood from the weak string in Figure 1. The function $u_{str}(x)$ is obtained by minimizing an energy function $E_{str}(u_{str}, d_{str})$. The problem can be converted into a discrete problem by finite elements[46]. In the discrete form, the energy function can be expressed as

$$E_{str} = D_{str} + S_{str} + P_{str} \quad (5)$$

where

$$\text{Measure of faithfulness } D_{str} = \sum_{i=1}^{N} (u_{str_i} - d_{str_i})^2$$

$$\text{Stretching energy } S_{str} = \lambda_{str}^2 \sum_{i=1}^{N-1} (u_{str_i} - u_{str_{i+1}})^2 (1 - l_{str_i})$$

$$\text{Penalty } P_{str} = \alpha_{str} \sum_{i=1}^{N-1} l_{str_i} \quad (6)$$

Here λ_{str} is the string elasticity and the parameter is used to control the scale of reconstruction. In the energy calculation, the penalty parameter, α_{str} is incorporated at the point of discontinuity. l_{str_i} is the boolean variable and $l_{str_i} = 1$ at the point of discontinuity, otherwise $l_{str_i} = 0$.

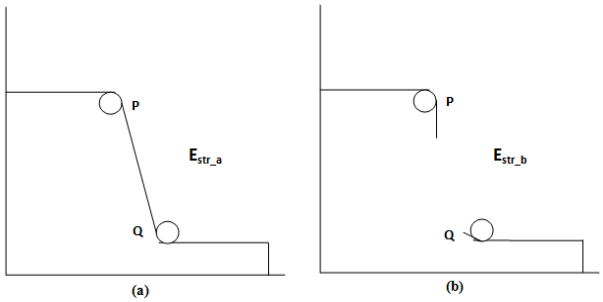

Figure 1. The weak string shown in figure is breakable in position PQ. (a) The string is continuous with energy E_{str_a} (b) The string is broken(discontinuous) with energy E_{str_b}. Position of sting in (a) is stable when $E_{str\_a} < E_{str\_b}$ and position of string is stable in (b) when $E_{str\_b} < E_{str\_a}$

B. Proposed energy function for segmentation based on IT2FS and weak continuity constraints

The segmentation of image I means division of pixel values in a number of disjoint classes depending on some features. Mathematically, it can be said as a mapping function $v : I \rightarrow R$ where R denotes the group of all pixels and R_1, R_2....R_c are the c segments then

$$R = R_1 \bigcup R_2 \bigcup .... \bigcup R_c \quad (7)$$

such that $R_1 \bigcap R_2 .. \bigcap R_c = \phi$. Within each segment R_i, the pixel values are either constant or vary very slowly i.e they are continuous within a segment. Moreover, the variation of the pixel values would be high at the boundary between the two segments i.e at the point of discontinuity between the segments. Thus, the R is continuous at every point except at the boundaries where it should violate the weak continuity constraints. The energy function E which can incorporate the knowledge of discontinuities in the segmentation process is defined as follows

$$E = D + S + P \quad (8)$$

where

$$D = \sum_{i=1}^{c} \sum_{x \in R_i} (x - v(R_i))^2$$

$$S = \lambda^2 \sum_{i=1}^{c} \sum_{x \in R_i} \sum_{y \in N_x} (\mu(x) - \mu(y))^2 (1 - l(x))$$

$$P = \alpha \sum_{i=1}^{c} \sum_{x \in R_i} l(x) \quad (9)$$

Now, E can be rewritten as

$$E = \sum_{i=1}^{c} \Big\{ \sum_{x \in R_i} (x - v(R_i))^2 + \lambda^2 \sum_{x \in R_i} \sum_{y \in N_x} (\mu(x) - \mu(y))^2 (1 - l(x)) + \alpha \sum_{x \in R_i} l(x) \Big\} = \sum_{i=1}^{c} E_{R_i} \quad (10)$$

In the above equation E_{R_i} is the energy of the segment R_i, $v(R_i)$ is the center of gravity (COG) of IT2FS representing the segment R_i. $\mu(x)$ is the membership value of the pixel x and N_x is a set of neighborhood pixels within a local window of size $\lambda \times \lambda$. The $l(x) = 1$ at the point of boundary between the segments and at the non-boundaries $l(x) = 0$. S and P quantity of the equation represent the spatial feature of the image in the segmentation process. Accurate segments $R_i, i = 1,2..c$ are obtained when the energy E is minimum. The energy function acts as the objective function in the segmentation process. Visual realization of two clusters with the COG $v(.)$, scale parameter λ , penalty parameter α and weak continuity regions are shown in Figure 2.

The Eq (10) represents the total energy when the number of segments in an image is c. In the process of thresholding an image $I = [x_{min}\ x_{max}]$ is divided into two segments (i.e $c = 2$) by a threshold t. They are background $I_b = [x_{min}\ t]$ and object $I_o = [t+1\ x_{max}]$. If the total energy is denoted by E_t and the energies of I_b and I_o are as E_{t-} ,E_{t+} respectively, then E_t can be written from Eq (10) as $E_t = E_{t-} + E_{t+}$. The threshold t for which E_t is minimum will give the accurate segmentation.

C. Importance of weak continuity constraints in the segmentation by thresholding

It is already mentioned in Section II-A that a threshold t generates two segments in an image. A segmentation boundary between the segments is the locations where two neighboring pixels with intensities x_1, x_2 will have $x_1 \leq t$ and $x_2 > t$ or vice versa. In the proposed method, we consider the segmentation boundaries as the position where weak continuity constraints are violated with the simultaneous detection of segments and localization of segmentation boundaries. In the non-boundary positions, the constraints are not violated. With these considerations, we apply the theory of weak continuity constraints for the segmentation and it seems appealing and convenient. The weak continuity constraints are violated as there is a change of average intensity levels from one segment to another. The violation is given importance in the proposed method by penalty P. Quantitatively, the weak continuity constraints are measured by the change of neighborhood membership values in the proposed method. When the change is high the continuity is weak and vice versa. Moreover, the locations where the weak continuity constraints are not violated are given importance by the quantity of S in the proposed method. As per the theory of weak continuity constraints in a string, proper localization of discontinuities results in the stability of the string with minimum energy. Similarly, in a segmentation process, accurate segmentation boundaries are detected with the minimization of energy. We discuss in details the terms D, S and P in the context of segmentation in Section III-D.

As already mentioned that for proper segmentation of an image, one should handle the uncertainties in the segmentation process. In the proposed method we minimize an energy function to generate the accurate segments of an image. Thus, it is necessary to establish a relation between the energy function and the uncertainties in the segmentation process. In the following proof, we show the relationship between the uncertainty in the segmentation process and the proposed energy function and it shows minimization of the energy is necessary for proper segmentation.

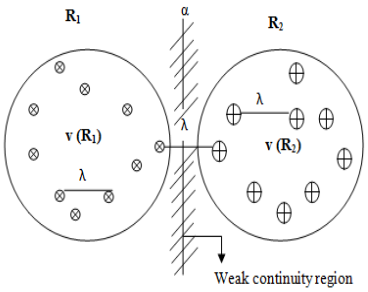

Figure 2. Visualization of two clusters with the cluster center $v(.)$, scale λ and penalty α. The continuity constraint is violated in the weak continuity region with penalty α

Theorem 1: The uncertainty in the segmentation will be minimum when E is minimum.

Proof: Let us consider the two accurate segments R_1 and R_2 of an image $I = [0\ 1]$ as shown in Figure 3(a)(Top). The classes/clusters are true classes and the two classes occur due to true threshold t. In the figure 3(a)(Bottom), the vertical axis represents corresponding average intensity of classes along the rows and the horizontal axis represents the positions of the intensity values. Figure 3(b) shows the segmentation due to the improper threshold t' with the corresponding classes R'_1 and R'_2. That means, in Figure 3(a) the data points in a segment are smooth or almost continuous everywhere except at the position of the boundary between the two segments R_1 and R_2. Thus, as per the theory of weak continuity constraints the weak continuity will be violated at the position of boundary between the segments and it will produce minimum energy at t. That means $E_t < E_{t'}\ \forall t' \in [0\ L]$ and $t \neq t'$,where E_t,$E_{t'}$ are the energies due to discontinuity at t and t' respectively. Since, the segmentation in Figure 3 (a) is accurate, the contrast among the regions R_1 and R_2 is the highest. Thus, the difficulty(ambiguity) in taking decision about the segmentation boundary in minimum. As a result uncertainties U_t occur due to ambiguities are minimum when threshold is t. On the other hand the ambiguity in the regions R'_1 and R'_2 will be high due to the presence of misclassified region as shown in Figure 3(b). This misclassification makes the contrast among the regions R'_1 and R'_2 low and it also makes the homogeneity among the pixels in R'_2 low. Thus, the boundary between the regions is not true segmentation boundary and uncertainty $U_{t'}$ is high. Thus it is evident $U_t < U_{t'}\ \forall t' \in [0\ L]$ and $t \neq t'$. So, it can be said whenever E_t is minimum, U_t will be minimum. Hence the proof.

D. Analysis and Generation of D, S and P for segmentation

In the Eq (9), the D represents the total sum of the square of the distance of each pixel within a segment R_i from the center of gravity(COG) $v(R_i)$ of the corresponding IT2FS. The COG represents the average of all centroids of all the embedded sets in IT2FS. The COG is chosen as a representative value or cluster center of the segment. It has a nice property of

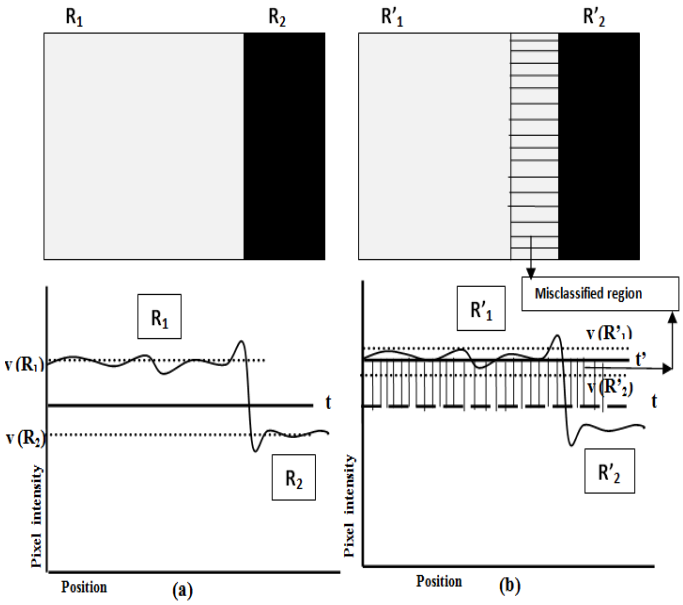

Figure 3. Two class segmentation of an image I by the proposed method with (a)Top: Segmentation into R_1 and R_2 by the proper threshold value t. Bottom: Average intensity values of the proper segments along rows and threshold t (b)Top: Segmentation into R'_1 and R'_2 by the improper threshold value t'. Bottom: Average intensity values of the proper segments along rows and threshold t'

drifting away from an uncertain zone to a certain zone [50]. Thus, D represents the gray level ambiguity present in the image and minimization of E minimizes the ambiguity. For the evaluation of COG, we use Nie-Tan operator proposed by Nie et al.[51]. In this method, a representative embedded type-1 fuzzy set of the IT2FS is found out whose centroid is equivalent to the COG of the IT2FS. The representative embedded type-1 membership value from the IT2FMF value is computed as $\mu = \frac{\overline{\mu}+\underline{\mu}}{2}$. This is followed by the computation of the centroid in discrete case by

$$v(R_i) = \frac{\sum_{x_{min}}^{x_{max}} \mu(x).xdx}{\sum_{x_{min}}^{x_{max}} \mu(x)dx} \tag{11}$$

Nie-Tan operator produces crisp output and it is the exact representation of the COG of IT2FS. The computational complexity of the COG by the operator is low and it is very efficient for practical application [52].

The term S represents the change of membership values over a neighborhood of a scale λ. In the proposed method, a local overlapping window of size $\lambda \times \lambda$ is taken in the image and average membership difference of the neighborhood pixels from the center pixel of the window is computed for S. The membership values used for the S are the values of the representative embedded type-1 fuzzy membership values within the window. The $l(x)$ is a boolean value as described in the previous section. The term S incorporates the spatial information of the segments except at the boundary regions. Thus, it represents the spatial ambiguity present the image.

The scale parameter λ helps to capture the texture of different segments in an image. There is a tradeoff between the high and low value of λ. A low value of λ cannot capture the texture of the different clusters/classes properly. On the other hand, a high value of λ may introduce more uncertainties in the segmentation process by mixing the properties of two different clusters[53]. To select the proper size of λ we use the concept of spectral flatness measure(SFM)[54] of an image. The SFM is the ratio of the arithmetic mean and geometric mean of the Fourier coefficients of the image. The SFM nearer to 1 means the image has a lot of edges and the λ should be low. Again, λ should be high when SFM is nearer to 0.

The penalty P is related to the boundary points i.e the point where weak continuities in the segments are violated. The P term also represents the spatial ambiguity in the image. When α is low it may detect spurious discontinuities in a segment.

The penalty parameter α helps to localize the discontinuities in the segmentation boundaries. When the contrast among two neighborhood segments is high (i.e weak continuity) the α should be low to make the energy E low to detect the discontinuities. Otherwise, α should be high to prevent the detection of wrong discontinuities by making the energy E high. In the proposed method the value of α is selected depending on the average difference of the type-reduced membership values of the neighborhood pixels in the boundary between the segments. If the difference is more than 0.5 the α is considered low, otherwise, it is taken high. In the proposed method, a set of boundary pixels are given as $B(x,y) = \{x,y|x,y \text{ are adjacent and } x \leq t \& y > t \text{ or } x > t \& y \leq t\}$.

In the literature, Otsu's method[13] is one of the most popular benchmark conventional programs for segmentation using thresholding. A large number of methods are found to modify Otsu's methods for two class and multi-class image segmentation ([7], [14], [15]). So, the following proof shows the efficiency of the proposed method.

Corollary 1: Otsu's objective function is a special case of the proposed IT2FS based energy function

Proof: If we assume that no uncertainties exits in the segmentation process, we can consider the upper membership value $\overline{\mu}(x)$ and lower membership value $\underline{\mu}(x)$ are same(i.e the interval is zero). That means $\overline{\mu}(x) \approx \underline{\mu}(x) \approx k_i$ where k_i is a constant and $x \in R_i$. Then the type-reduced membership values using Nie-Tan operator is given by $\mu(x) \approx \frac{k_i+k_i}{2} = k_i$. Now putting the values in the Eq11 we have COG $v(R_i) = \frac{\sum_{x \in R_i} x\mu_i(x)}{\sum_{x \in R_i} \mu_i(x))} = \frac{\sum_{x \in R_i} xk_i}{\sum_{x \in R_i} k_i} = \bar{x}$. Moreover, if we do not consider any spatial and boundary information we can take $S = 0$ and $P = 0$. So, the Eq 8 can be written as

$$E = D = \sum_{i=1}^{c} \sum_{x \in R_i} (x - \bar{x})^2 \tag{12}$$

If $c = 2$ the above equation can be written as

$$E = \sum_{x \in R_1} (x - \bar{x})^2 + \sum_{x \in R_2} (x - \bar{x})^2 \tag{13}$$

The above E will be minimum when $E' = E/N$ is minimum where $N = N_1 + N_2$. N_1,N_2 are the number of pixels in R_1, R_2 and N is the total number of pixels. Now,

$E' = \frac{\sum_{x \in R_1} (x-\bar{x})^2 + \sum_{x \in R_2} (x-\bar{x})^2}{N}$

$= (\frac{N_1}{N}) \frac{\sum_{x \in R_1} (x-\bar{x})^2}{N_1} + (\frac{N_2}{N}) \frac{\sum_{x \in R_2} (x-\bar{x})^2}{N_2}$

$= w_1\sigma_1^2 + w_2\sigma_1^2$

So, $E' = w_1\sigma_1^2 + w_2\sigma_1^2$ where $w_1 = N_1/N$, $w_2 = N_2/N$ are the

class probability of R_1,R_2 and σ_1^2, σ_2^2 are the variances of the segments R_1,R_2. E' is the Otsu's objective function for object-background segmentation and it represents the sum of intra-class variance of the different segments. Hence the proof. So, it can be said for two class segmentation when no uncertainty is considered in the image, and spatial and boundary information are ignored the proposed energy function reduces to Otsu's objective function.

The penalty parameter α is a measure of noise immunity of the thresholding method. When the value of α is very low, noise may produce undesired or spurious discontinuities in the segment. The following corollary shows that the low value of α may detect spurious discontinuities in a segmentation.

Corollary 2: The segmentation result will not detect any spurious discontinuities in a segment of image I provided $\alpha p_{min} > D_{L_m}/n - \sigma_I^2 + \lambda^4$ *where the image* $I = [0\ L_m]$, $p_{min} = n_{min}/n$, *where* n_{min} *is the minimum non zero frequency of pixel in the image,* D_{L_m} *is the measure of faithfulness of the segment,* σ_I^2 *is the variance of the image, and n in number of pixels in the image.*

Proof: Let us assume an image I has only one class in it. The method will detect one class with no discontinuities in the image only when threshold $t = L_m$. Thus, $D_{L_m} + S_{L_m} + P_{L_m} < D_x + S_x + P_x,\ \forall x \in [0\ L_m]$. Since, there are no discontinuities in the segment of the image, so we have $P_{L_m} = 0$. The maximum value of S_{L_m} is given by $max\{S_{L_m}\} = \lambda^2 \times \lambda^2 \times n$. The reason is that maximum difference in membership values is 1 and there are λ^2 such values in a window of size $\lambda \times \lambda$ and the image has n pixels. Again the minimum value of D_x is $n\sigma_I^2$ where σ_I^2 is the variance of I. So, we can write
$D_{L_m} + \lambda^4 n < n\sigma_I^2 + S_x + \alpha n_1$,
n_1 is the number of discontinuities detected due to x. Since, the minimum value of $S_x = 0$,the above inequality must be satisfied $\forall x$ if
$D_{L_m} + \lambda^4 n < n\sigma_I^2 + \alpha n_1$
$\Rightarrow D_{L_m} - n\sigma_I^2 + \lambda^4 n < \alpha n_{min}$
$\Rightarrow D_{L_m}/n - \sigma_I^2 + \lambda^4 < \alpha(n_{min}/n)$
$\Rightarrow D_{L_m}/n - \sigma_I^2 + \lambda^4 < \alpha p_{min}$
From the above result it is evident that for very low value of α the inequality may not be satisfied and the spurious discontinuities will be detected.

IV. Iterative scheme for multi-class segmentation & algorithm

As already mentioned, in the proposed method no prior knowledge about the number of segments or classes is used. The method is fully automatic and can determine the optimal number of segments at the runtime of the process. Due to a threshold t an image $R = [x_{min}\ x_{max}]$ is segmented into two clusters (i.e c=2) denoted by background $I_b = \{x_{min}, 2, .., t\}$ and object $I_o = \{t+1, t+2, .., x_{max}\}$. Here, we denote the total energy generated due to the segmentation by the threshold t using E_t. The energy of the segments I_b, I_o are given by E_{t-} and E_{t+} respectively i.e $E_t = E_{t-} + E_{t+}$. The cluster centers of background I_b and object I_o are represented by v_{t-} and v_{t+} respectively. The cluster centers are computed by Nie-Tan operator described in Section III-D. In the proposed method at

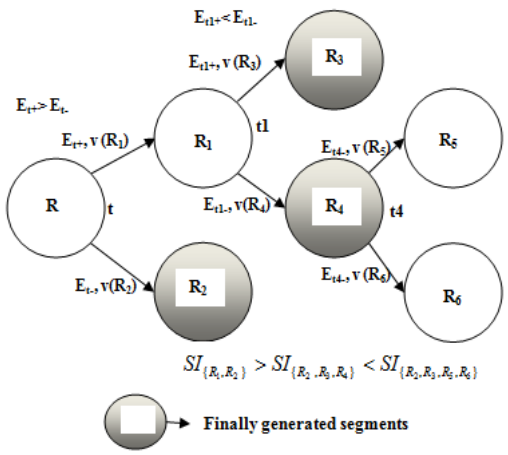

Figure 4. Tree structure for automatic multi-class segments R_2, R_3 and R_4 generations where $R = R_2 \bigcup R_3 \bigcup R_4$

first, the proper threshold t is found such that E_t is minimum and $t \in R$. Out of the two segments, the segment which has the greater energy is selected for further object-background segmentation. The iterative process will generate a binary tree structure. That means, in each level, a new set of segments are generated. For the iterative process, we have to take a decision whether the set of segments generated in the current level is better than that of the previous level or not. If the current set of segments is better than that of the previous level, the process will go for further iteration. Otherwise, the iteration will be stopped. The measure for taking the decision that a set of segments is better than another set of segments is given by segmentation index SI in the proposed method. The process continues until a base condition is satisfied. The base condition is that the iterative process will be stopped if the $SI_{K_j} < SI_{K_{j+1}}$ where K_j is the set of the segments in jth level and K_{j+1} is the set of segments generated in $j+1$th level and SI is segmentation index. The segmentation index is defined as

$$SI_K = \frac{\sum_{i=1}^{c} E_{R_i}}{var(v(R_1), v(R_2), ..., v(R_c))} \tag{14}$$

In the above equation E_{R_i} is the energy of a segment R_i and $K = \{R_1, R_2, .., R_c\}$. R_i has the cluster center $v(R_i)$ and $var(.)$ is the variance. The energy of segment R_i is given by Eq (10). From, the theory of weak continuity constraints it is logical to say that the individual segments should attain minimum energy after detecting the accurate segmentation boundaries. Thus, for proper segmentation the total energy i.e $\sum_{i=1}^{c} E_{R_i}$ should be minimum. Moreover, from the segmentation point of view the variance between the cluster centers i.e $var(v(R_1), v(R_2), ..., v(R_c))$ should be maximum. Thus, the attainment of the minimum SI_K indicates the proper generation of the segments. If T is the set of thresholds which generates R_is and c is the number of the current segments i.e $i = 1, 2, .., c$ then $c = |T| + 1$. Since the number of thresholds points are finite and one threshold cannot be repeated, the algorithm will converge after a finite amount of time. The proposed technique is shown in Algorithm 1.

The iterative segmentation process can be explained by the tree structure shown in Figure (4). In the figure at

first the image R is divided into the segments R_1(object) and R_2(background) by the threshold t where $E_{R_1} = E_{t+}$, $E_{R_2} = E_{t-}$ and E_t is minimum and $t \in R$. Assuming $E_{t+} > E_{t-}$ i.e $E_{R_1} > E_{R_2}$, R_1 will again be divided into the segments R_3(object) and R_4(background) by threshold $t_1 \in R_1$. Since, from the figure $SI_{\{R_1,R_2\}} > SI_{\{R_2,R_3,R_4\}}$ iteration will go for the next level as described in Algorithm1. In the next level the segments are R_2, R_3, R_5, R_6 and $SI_{\{R_2,R_3,R_4\}} < SI_{\{R_2,R_3,R_5,R_6\}}$. That means the base condition is satisfied and the iteration will be stopped. The final generated segments will be R_2, R_3, R_4.

Input: The gray level image I.
Output: Multi-class segmentation by a set of thresholds T.
Initialisation : $T = \{\phi\}$ $flag = 1$,$SI_{mod} = 0$
$x_{min} = min\{x|x \in I\}$,$x_{max} = max\{x|x \in I\}$. Initialize λ by SFM of I. // SI_{mod} **is** SI **at previous level**
1: **for** $t = x_{min}$ to x_{max} **do**
2: Transform the image pixels from $x = x_{min}$ to $x = x_{max}$ into T1FS by the Eq 3.
3: Compute the IT2FS from the T1FS by the Eq 4.
4: Find the centroid v_{t-} for the set $[x_{min}\ t]$ and v_{t+} for the set $[t+1\ x_{max}]$ using Nie-Tan operator to compute D. Evaluate the terms S and P using the parameters λ and α for both sets.
5: Calculate E_{t-} and E_{t+} by Eq (10)
6: Compute $E_t = E_{t-} + E_{t+}$.
7: **end for**
8: Find t for which E_t is minimum.
9: Compute SI_K // SI_K **is** SI **at current level**
10: **if** $(flag = 1)$ **then**
11: $SI_{mod} = SI_K + 1; flag = 0$ // **Initialization of** SI_{mod}
12: **end if**
13: **if** $(SI_K < SI_{mod})$ **then**
14: $SI_{mod} = SI_K$, // **Checking base condition**
15: **else**
16: Goto END.
17: **end if**
18: $T = T \bigcup \{t\}$,
19: **if** $(E_{t-} > E_{t+})$ **then**
20: Put $x_{max} = t$ and goto step 1.// **Segmentation of region** $\{x_{min}, 2, .., t\}$
21: **else**
22: Put $x_{min} = t+1$ and goto step 1.// **Segmentation of region** $\{t+1, t+2, .., x_{max}\}$
23: **end if**
24: END: Segment the image by the thresholds T.

Algorithm 1: Algorithm for automatic multi-thresholding by the proposed method. Here K is the set of segments generated by T.

V. Performance Measure of the Proposed Method

The quantitative performance of the proposed thresholding method and all the methods compared here are measured using five different quantitative measures. They are Segmentation Accuracy(S.A)[55], Misclassification error(M.E) [56], Rand index(RI)[57], Global Consistency Error (GCE)[57] and Fuzzy evaluation(FE)[58]. The correctly classified pixels with respect to the total number of pixels are measured by S.A. The M.E evaluates the performance of a segmentation method in terms of Multi-class type-I error. It is based on number of mis-segmented pixels. The average value of M.E lies between 0 and 1. The low M.E indicates good performance. When the segmented image is close to the ground truth the RI index tends to 1, otherwise, it tends to 0. it The GCE measures the similarities between the segmented image and its ground truth and has a value between 0 and 1. When the segmented image is similar to ground truth the GCE tends to 0. In FE, a fuzzy-based technique is used to compute the F-score.

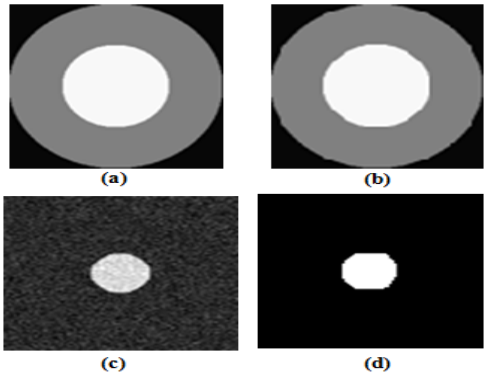

Figure 5. (a) Original synthetic test image with 3 class (b) Result by the proposed method (c) Image corrupted by white Gaussian noise of variance .01 (d) Result by the proposed method

Though we measured the performance of all the methods considered here using different measures, it is a fact [59] that performance of segmentation evaluation methods depends on the image content which may vary widely. Therefore, it is more logical to find out the statistical performance bound of a segmentation method associated with a particular image content. The measure should give an upper bound of the performance achievable by a segmentation algorithm on the particular image. Hence, to statistically bound the performance of our multi-thresholding method a modified Cramer-Rao bound(CRB) on Mean Square Error(MSE) for segmentation was used. It was developed by Peng et al.[60].

VI. Experimental Results & Discussion:

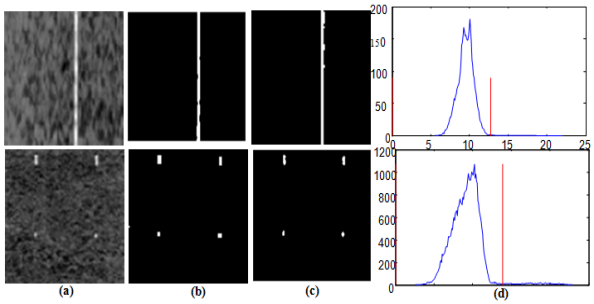

Figure 6. (a) NDT test image (b) Ground truth (c) Segmentation results by the proposed method (c) Histogram of the image with the threshold point

To exhibit the performance of the proposed method we tested our method on different types of images. It is to be

noted that we considered only the gray level pixel intensity as a feature for segmentation. We applied our method on synthetic images[61] and the benchmark dataset of the camera captured natural images from Weizmann[62], and Berkley[63]. The non-destructive testing images(NDT) from [64] and several brain MRI images from BrainWeb[65] and Oasis-brain dataset[66] were also used for the experiment. The size of the images varies from 200×200 to 500×500. The dataset [64] contains images which have two classes in them. The dataset [63],[65],[66] contain multi-class images and dataset [62] has both the two-class and multi-class images. We compared the performance of the proposed method both qualitatively and quantitatively with conventional methods like Otsu[13], Cai[7], Singla[16], Wang[17], a type-1 fuzzy set based method like Bustince[30] and type-2 fuzzy-based method like Tizhoosh[40] and Dhar [41]. For the performance measure the ground truth were available with the mentioned dataset. For the brain images from Oasis-brain dataset we took the help of the expert also. MATLAB2013 with 8GB RAM were used for the experimental verification.

For qualitative and quantitative performance comparison with different methods, we considered both the two-class segmentation(i.e $|T| = 1$) techniques(e.g. Otsu, Bustince, Tizhoosh, Dhar) and multi-class segmentation(i.e $|T| > 1$) techniques(e.g. Cai, Singla, Wang). It is obvious that two class segmentation is a special case of multi-class segmentation, where the class number is two. We applied the proposed method on two class images to compare with the two-class segmentation techniques. We also applied the proposed method on multi-class images for comparison with the multi-class segmentation techniques. If the proposed method detected more or less number of segments/classes in an image than that of corresponding ground truth, the detection was considered as over-segmentation or under-segmentation respectively. The over-segmentation and under-segmentation by the proposed method were evaluated by the measure in [67]. The average over-segmentation and average under-segmentation performance of the proposed method in a range $[0\ 1]$ were found to be 0.15 and 0.11 for the datasets described above. In a general situation, a method like Otsu which is considered as one of the benchmark methods for segmentation is faster than the iterative methods. But, here our intention was to compare the quality of results, not the computational cost.

A. Experiments on synthetic images

The proposed method was applied to the synthetic test images as shown in Figure 5(a). The circular synthetic image had three classes with pixel intensities 34,100 and 230. No prior knowledge about the number of segments was given and the method automatically detected the number of classes and segment it (Figure 5(b)). It can be seen from the result that the proposed method segmented the synthetic image accurately.

The performance of the proposed method under noise corruption is shown in Figure 5(d). The synthetic image was corrupted by the white Gaussian noise of variance .01(Figure 5(c)). The noise corruption injected more uncertainties in the image. The centroid of the IT2FS moved in accordance to the uncertain zone to handle the injected uncertainties properly. As already described, it moves away from an uncertain zone to a certain zone to reduce the uncertainties in the segmentation process. Moreover, the weak continuity constraints were not violated in the noisy pixels and so, no spurious discontinuities were detected. Thus, the IT2FS based proposed method reduced the gray level, spatial ambiguities and the boundaries of the segments were detected properly.

Table I
QUANTITATIVE PERFORMANCE OF DIFFERENT METHODS ON THE NDT IMAGES FROM [64]. ↑ MEANS HIGHER VALUES REPRESENT BETTER PERFORMANCE AND ↓ MEANS LOWER VALUES REPRESENT BETTER PERFORMANCE

Image	Otsu	Cai	Bustince	Tizhoosh	Dhar	Proposed
SA↑	0.7831	0.8023	0.7771	0.7921	0.8301	0.9016
M.E↓	0.2354	0.1132	0.1982	0.1418	0.0408	0.0291
GCE ↓	0.4111	0.3702	0.3521	0.2700	0.2144	0.1001
RI ↑	0.7611	0.7702	0.7501	0.7700	0.8105	0.8990
FE ↑	0.7451	0.7413	0.8221	0.8273	0.8502	0.9023

B. Experiments on highly uncertain NDT images

In this section, we applied the proposed method on NDT images which possess high gray and spatial level ambiguity. NDT is used in the industry to test a metallic object without destroying it. Industries nowadays use computer vision techniques to detect the fault in the object. But, the segmentation of faulty regions from the background in those images is quite difficult. The histograms of an NDT image is either unimodal or there is no clear valley between the two different modes(Figure 6). Obviously, they are difficult to segment. We applied the proposed method to distinguish the object from the background in the NDT images as shown in Figure 6. The quantitative evaluation of the proposed method and all other methods using SA, M.E,GCE, RI, and FE are shown in Table I. From the quantitative evaluation, it can be said the proposed methods performed better compared to the other methods. The boundaries between the segments were located even in the low difference of membership values. The method by Otsu minimized the intra-class variance to find the boundaries between the segments. But it ignored the high uncertainties related with the NDT images in the boundary regions. We have proved in Section III-D that the Otsu's method is a special case of the proposed IT2FS based method when no uncertainties are considered. The method by Cai first used the Otsu's method to find the initial threshold and then found 'to-be-determined'(TDT) zone for further segmentation. The method also did not handle the uncertainties and number of classes were ad-hoc or fixed. The method by Bustince used type-1 fuzzy set for uncertainty handling which is less powerful compared to the IT2FS for handling the uncertainties. Moreover, it had no provision for handling discontinuities at the boundaries by incorporating the neighborhood information. Tizhoosh[40] and Dhar[41] used IT2FS for uncertainty handling. Both Tizhoosh and Dhar minimized type-2 fuzzy entropy for threshold generation. But, all of them ignored the uncertainties prevailed at the boundary regions of the segments. On the other hand, the proposed method calculated

This article has been accepted for publication in a future issue of this journal, but has not been fully edited. Content may change prior to final publication. Citation information: DOI 10.1109/TFUZZ.2019.2930932, IEEE Transactions on Fuzzy Systems

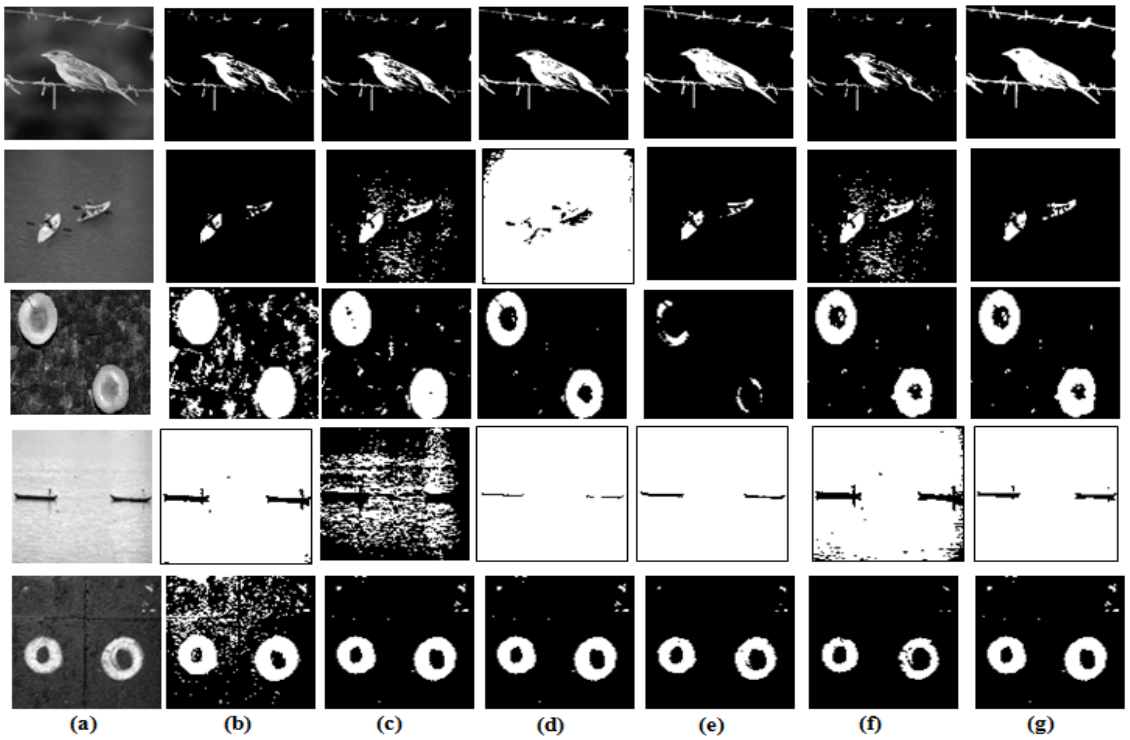

Figure 7. Column-wise(a) Original test image. Segmentation results (b)Otsu (c)Cai (d)Bustince (e)Tizhoosh (f)Dhar (g)Proposed

the minimum energy function using the IT2FS and weak continuity constraints. The method minimized the uncertainties due to gray level and spatial ambiguities, and thus detected the boundaries with simultaneous localization.

Table II
QUANTITATIVE PERFORMANCE OF DIFFERENT METHODS ON THE NATURAL IMAGES FROM [62]

Image	Otsu	Cai	Bustince	Tizhoosh	Dhar	Proposed
SA↑	0.8051	0.8203	0.8215	0.8342	0.8425	0.8892
M.E↓	0.1056	0.1044	0.0917	0.0844	0.0943	0.0801
GCE ↓	0.4020	0.3622	0.3314	0.3200	0.2041	0.1902
RI ↑	0.8121	0.8104	0.8321	0.8705	0.8725	0.9021
FE ↑	0.7611	0.8211	0.8011	0.8224	0.8402	0.9412

C. Experiments on natural images

We tested the proposed method on the natural images from [62] in this subsection. The dataset contains 100 images for two class segmentation and 100 images for multi-class segmentation. The image size varies from 200×200 to 500×500. The uncertainties in natural images are more due to inherent noise corruption in the image during the capturing of the image and also due to analog to digital conversion. Another difficulty with a natural image is that it is very difficult to determine the correct number of segments in the image without having a prior knowledge. Figure 7 shows the segmentation results of the natural images by the proposed method and the other methods. It is to be noted that the other methods compared here (Figure 7) had the knowledge

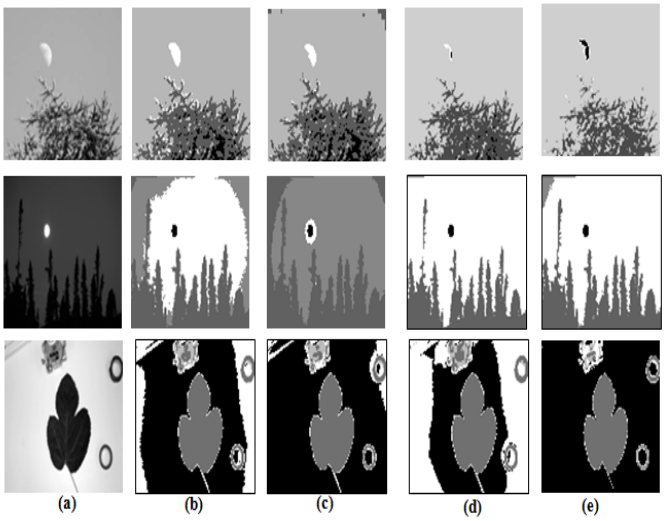

Figure 8. Multi-thresholding results in column-wise (a) Original test image. Segmentation results by (b)Singla (c)Cai (d)Wang (e)Proposed method.

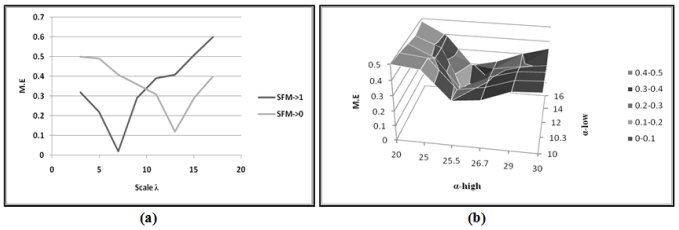

Figure 9. (a) Average values of M.E with different values of λ. (b) Variations of average M.E with different values of $\alpha - low$ and $\alpha - high$

about the number of segments. The results indicate that the proposed method was quite capable of segmenting the natural images as well. The reason is that the IT2FS has a powerful uncertainty handling capacity with the boundary detection techniques than that of the other methods compared here. The quantitative performance of the proposed method and all the methods compared here are shown in Table II.

Here, we also compared the performance of the proposed method with the methods by Singla[16] and Wang[17] which were also capable of automatic multi-class segmentation. Both the methods used the energy function minimization techniques to get multi-class segmentation. But they had no uncertainty handling tool incorporated into their energy functions. The images tested here had more than two segments. From the visual inspection of the qualitative results in Figure 8 it can be seen that automatic thresholding for multi-class segments generation by the proposed method was more capable than the methods in [16] and [17]. Though the methods by Singla and Wang were able to recognize the number of classes but due to lack of proper uncertainty handling capacity the average performances were low. Moreover, Wang reduced the piecewise constant Mumford-Shah energy function to get the segmented image and the process involved a convolution step to find a perimeter value in the energy function. This step might blur the boundaries and increased uncertainties.

D. Determination of the parameters β, λ and α

In this subsection, we studied the three parameters used in the experiments. As already stated the parameter β was used to generate the IT2FM from type-1 fuzzy membership function where $\beta \in (1, \infty)$. Now, it was found experimentally by [40] that the value of $\beta \gg 2$ was not very useful for image data. So, following the strategy of [40] we considered the value of $\beta = 1.25$ throughout the experiments. In Section III-D it is mentioned that λ should be chosen depending on the SFM. The average M.E for NDT images with different scales for the high value of SFM and low value of SFM are shown in Figure 9(a). Thus, the $\lambda = 7$ for high SFM and $\lambda = 13$ for low SFM were found to be appropriate for NDT images used here. The same values of λ were used for all the experiments. Similarly, the values of $\alpha - low$ for weak continuity and $\alpha - high$ for strong continuity with M.E on the NDT images are shown in Figure 9(b). From the curve, it was found the $\alpha - low = 14$ and $\alpha - high = 25.6$ were appropriate for the images considered here.

E. Experiments on Kaggle2018 dataset

In this subsection we tested the proposed method on complex nuclei images from Kaggle2018 dataset[68]. The dataset contained a variety of biological images. Here, the nuclei images were derived from several living beings like humans, mice, and flies. The images were taken in different conditions like fluorescent and varying illuminations etc. The uncertainties in the image patterns were high as evident from the visual inspection of the images shown in Figure 10. From the figure we can find the qualitative performance of the proposed method. The results show the segmentation boundaries. From visual inspection it is evident that the proposed method not only correctly detected the segments but also localized the boundaries accurately. The quantitative performance comparisons with Singla [16],Cai[7], Wang[17] and Li[28] are shown in Table III. From the results it can be said that on average the proposed method performed better than the methods compared here.

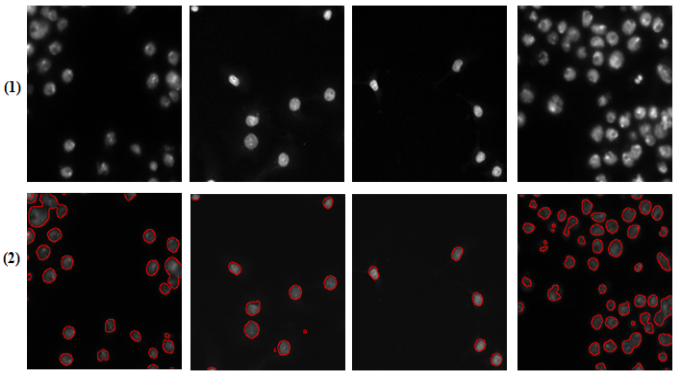

Figure 10. Row-wise (1) Original test nuclei images (2) Segmentation results by the proposed method with the segmentation boundaries

Table III
QUANTITATIVE PERFORMANCE OF DIFFERENT METHODS ON NUCLEI IMAGES FROM KAGGLE DATASET

Image	Singla	Cai	Wang	Li	Proposed
SA↑	0.8100	0.8178	0.8832	0.8943	0.9213
M.E↓	0.6241	0.5749	0.3211	0.2865	0.0132
GCE ↓	0.4236	0.3891	0.3271	0.2384	0.1761
RI ↑	0.8385	0.8611	0.9011	0.9102	0.9841
FE ↑	0.6512	0.7537	0.8001	0.8700	0.9184

F. Experiments on medical images

In this subsection, we tested the proposed method on medical images. For experiments on medical image segmentation, we tested the methods on brain MRI image from [65] and [66]. The dataset [66] contains a set of cross-sectional collection of 416 subjects aged 18 to 96. From the images, the first 100 images were taken for the performance measure. In clinical applications, the brain MRI segmentation is an essential task to detect the abnormality in the brain. This is because different processing steps rely on accurate segmentation of anatomical regions. The high uncertainties in a medical image are due to the lack of clear boundaries between the segments, the different type of noises and low contrasts between the segments. There are three regions in a brain MRI image. The regions are Grey matter (GM), White matter (WM) and cerebrospinal fluid (CSF). The proposed method automatically detected the regions accurately without any prior knowledge. The qualitative comparisons of the proposed method with the other methods are shown in Figure 11. The colors for different regions are used to distinguish the regions clearly. The average quantitative performances of the methods are shown in Table IV.

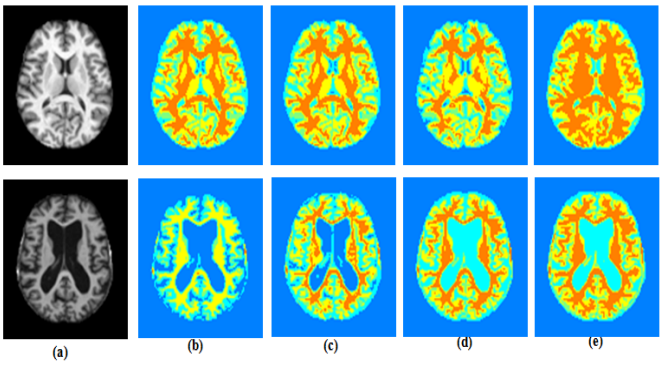

Figure 11. Segmentation results on the brain images (a) Original test image. Segmentation results by (b)Singla (c)Cai (d)Wang (e)Proposed method.

Table IV
QUANTITATIVE PERFORMANCE OF DIFFERENT METHODS ON THE MRI BRAIN IMAGES FROM [65]

Image	Singla	Cai	Wang	Proposed
SA↑	0.80211	0.8094	0.8771	0.9021
M.E↓	0.7031	0.6830	0.4302	0.1301
GCE ↓	0.4023	0.3632	0.3732	0.1353
RI ↑	0.8234	0.8502	0.9561	0.9569
FE ↑	0.6011	0.7212	0.7500	0.8712

G. Statistical validation by the modified Cramer-Rao bound for MSE

The robustness of the proposed method under noisy situation was measured statistically[60]. For this, we measured the lower bound for MSE on the Brain MRI image dataset. Here we assumed that each image had three non-overlapping basic regions ($M = 3$), GM, WM and CSF regions. Ground truths of the images were used for generating the three regions. The cubic B-spline function was used here to model the segmentation problem into a varying-coefficient model. The knots were set up at every 8 pixels in both the horizontal and the vertical directions. The images were corrupted with white Gaussian noise with zero mean and variance σ^2. This strategy was applied to all of the 100 MRI brain images in the dataset. Figure 12 shows the average lower bound of MSE with the average individual MSE at different SNRs. The performance of the proposed method is followed by Wang. This measure also indicates that the proposed method was more robust against the noise corruption compared to the other methods used here and it reduced the uncertainties due to the noise successfully. The proposed method ensured that in the noisy region the continuity constraints were not violated. No such noise-control was possible in the other methods compared here. The graph also gives the room for improvement of the proposed method.

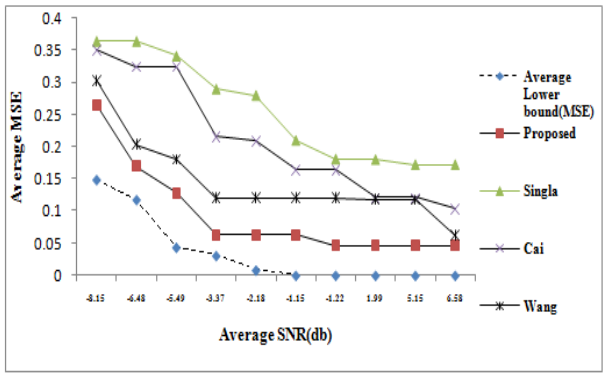

Figure 12. Average Modified CRB of a brain image with the different methods

VII. CONCLUSION

Uncertainties handling is a key problem in multi-class image segmentation. The IT2FS is a powerful uncertainty handling tool. But, the current measures of uncertainty do not take into consideration the boundary information. In this paper, we have proposed an IT2FS and weak continuity constraints based energy function for multi-class image segmentation. The IT2FS along with the weak continuity constraints concept is used to localize the boundaries between the segments and thus they help to reduce the gray level and spatial ambiguities in an image segmentation. The energy function acts as a measure of uncertainty in the IT2FS domain for image segmentation. The technique overcomes the limitation of fuzzy type-2 based objective functions to localize the segmentation boundaries with the help of a scale and penalty parameters involved with the weak continuity constraints. To get the appropriate set of threshold values the segmentation problem is treated as the energy minimization problem. The method automatically found the number of classes without a prior knowledge. The proposed technique is the generalization of the conventional Otsu's method. The method performed equally well for the synthetic, highly difficult NDT images, natural scene images, and medical images. It was found that under the noise corruption it also performed well. It was verified by the modified Cramer-Rao bound for the MSE. The method can be extended for the colour and complex texture segmentation problem, which is currently under investigation.

VIII. ACKNOWLEDGEMENT

We would like to thank Dr. Rahul Saha, Senior Resident(Neurosurgery), Park Clinic, Kolkata, India for helping us on Medical images.

REFERENCES

[1] J. F. Canny, "Finding edges and lines in images." MASSACHUSETTS INST OF TECH CAMBRIDGE ARTIFICIAL INTELLIGENCE LAB, Tech. Rep., 1983.
[2] M. Sezgin and B. Sankur, "Survey over image thresholding techniques and quantitative performance evaluation." *Journal of Electronic Imaging*, vol. 13, no. 1, pp. 146–165, 2004.
[3] R. Jain and R. S. Sharma, "Image segmentation through fuzzy clustering: A survey," in *Harmony Search and Nature Inspired Optimization Algorithms*. Springer, 2019, pp. 497–508.
[4] X. Cai, R. Chan, and T. Zeng, "A two-stage image segmentation method using a convex variant of the mumford–shah model and thresholding," *SIAM Journal on Imaging Sciences*, vol. 6, no. 1, pp. 368–390, 2013.
[5] M. Beauchemin, "Image thresholding based on semivariance." *Pattern Recognition Letters*, vol. 34, pp. 456–462, 2013.
[6] L. Zhao, S. Zheng, W. Yang, H. Wei, and X. Huang, "An image thresholding approach based on gaussian mixture model," *Pattern Analysis and Applications*, pp. 1–14, 2019.
[7] H. Cai, Z. Yang, X. Cao, W. Xia, and X. Xu., "A new iterative triclass thresholding technique in image segmentation." *IEEE Transactions on Image processing.*, vol. 23, no. 3, pp. 1038–1046, 2014.

[8] Y. Lai and P. Rosin., "Efficient circular thresholding." *IEEE Transactions on Image processing*, vol. 23, no. 3, pp. 992–1001, 2014.

[9] T. Wu, R. Hou, and Y. Chen, "Cloud model-based method for infrared image thresholding," *Mathematical Problems in Engineering*, vol. 2016, 2016.

[10] X. Zheng, H. Ye, and Y. Tang, "Image bi-level thresholding based on gray level-local variance histogram," *Entropy*, vol. 19, no. 5, p. 191, 2017.

[11] B. Wang, L. Chen, and J. Cheng, "New result on maximum entropy threshold image segmentation based on p system," *Optik*, vol. 163, pp. 81–85, 2018.

[12] P. Maji, M. K. Kundu, and B. Chanda, "Second order fuzzy measure and weighted co-occurrence matrix for segmentation of brain mr images," *Fundamenta Informaticae*, vol. 88, no. 1-2, pp. 161–176, 2008.

[13] N. Otsu., "A threshold selection method from gray level histograms." *IEEE transactions on System Man and Cybernatics.*, vol. 9, pp. 62–66, 1979.

[14] M. T. N. Truong and S. Kim, "Automatic image thresholding using otsuś method and entropy weighting scheme for surface defect detection," *Soft Computing*, pp. 1–7, 2017.

[15] F. Nie, P. Zhang, J. Li, and D. Ding, "A novel generalized entropy and its application in image thresholding," *Signal Processing*, vol. 134, pp. 23–34, 2017.

[16] A. Singla and S. Patra, "A fast automatic optimal threshold selection technique for image segmentation," *Signal, Image and Video Processing*, vol. 11, no. 2, pp. 243–250, 2017.

[17] D. Wang, H. Li, X. Wei, and X.-P. Wang, "An efficient iterative thresholding method for image segmentation," *Journal of Computational Physics*, vol. 350, pp. 657–667, 2017.

[18] S. Niu, Q. Chen, L. De Sisternes, Z. Ji, Z. Zhou, and D. L. Rubin, "Robust noise region-based active contour model via local similarity factor for image segmentation," *Pattern Recognition*, vol. 61, pp. 104–119, 2017.

[19] H. Yu, F. He, and Y. Pan, "A novel region-based active contour model via local patch similarity measure for image segmentation," *Multimedia Tools and Applications*, vol. 77, no. 18, pp. 24 097–24 119, 2018.

[20] L. Wang, G. Chen, D. Shi, Y. Chang, S. Chan, J. Pu, and X. Yang, "Active contours driven by edge entropy fitting energy for image segmentation," *Signal Processing*, vol. 149, pp. 27–35, 2018.

[21] J. Bragantini, S. B. Martins, C. Castelo-Fernandez, and A. X. Falcão, "Graph-based image segmentation using dynamic trees," in *Iberoamerican Congress on Pattern Recognition*. Springer, 2018, pp. 470–478.

[22] J. Pont-Tuset, P. Arbelaez, J. T. Barron, F. Marques, and J. Malik, "Multiscale combinatorial grouping for image segmentation and object proposal generation," *IEEE transactions on pattern analysis and machine intelligence*, vol. 39, no. 1, pp. 128–140, 2017.

[23] X. Dong, J. Shen, L. Shao, and L. Van Gool, "Sub-markov random walk for image segmentation," *IEEE Transactions on Image Processing*, vol. 25, no. 2, pp. 516–527, 2016.

[24] A. Pratondo, C.-K. Chui, and S.-H. Ong, "Robust edge-stop functions for edge-based active contour models in medical image segmentation," *IEEE Signal Processing Letters*, vol. 23, no. 2, pp. 222–226, 2016.

[25] C. Liu, W. Liu, and W. Xing, "An improved edge-based level set method combining local regional fitting information for noisy image segmentation," *Signal Processing*, vol. 130, pp. 12–21, 2017.

[26] S. Borjigin and P. K. Sahoo, "Color image segmentation based on multi-level tsallis-havrda-charvát entropy and 2d histogram using pso algorithms," *Pattern Recognition*, 2019.

[27] M. Naidu, P. R. Kumar, and K. Chiranjeevi, "Shannon and fuzzy entropy based evolutionary image thresholding for image segmentation," *Alexandria engineering journal*, vol. 57, no. 3, pp. 1643–1655, 2018.

[28] J. Li, W. Tang, J. Wang, and X. Zhang, "Multilevel thresholding selection based on variational mode decomposition for image segmentation," *Signal Processing*, vol. 147, pp. 80–91, 2018.

[29] O. Tobias and R. Sear., "Image segmentation by histogram thresholding using fuzzy sets." *IEEE Transactions on Image processing*, vol. 11, no. 12, pp. 1467–1465, 2002.

[30] H. Bustince, E. Barrenechea, and M. Pagola., "Image thresholding using restricted equivalence function and minimizing the measures of similarity." *Fuzzy Sets and Systems.*, vol. 158, pp. 496–516, 2007.

[31] M. Gong, Y. Liang, J. Shi, W. Ma, and J. Ma, "Fuzzy c-means clustering with local information and kernel metric for image segmentation," *IEEE Transactions on Image Processing*, vol. 22, no. 2, pp. 573–584, 2013.

[32] L. A. Zadeh, "Quantitative fuzzy semantics." *Information science.*, vol. 13, pp. 159–176., 1971.

[33] N. N. Karnik and J. M. Mendel., "Introduction to type-2 fuzzy logic systems." *Proceeding of International Conference on Fuzzy Systems.*, pp. 915–920., 1989.

[34] V. Singh, R. Dev, N. K. Dhar, P. Agrawal, and N. K. Verma, "Adaptive type-2 fuzzy approach for filtering salt and pepper noise in grayscale images," *IEEE Transactions on Fuzzy Systems*, vol. 26, no. 5, pp. 3170–3176, 2018.

[35] J. Mendel, R. John, and F. Liu., "Interval type-2 fuzzy logic system made simple." *IEEE transactions on Fuzzy systems*, vol. 14, no. 6, pp. 808–821, 2006.

[36] S. Majeed, A. Gupta, D. Raj, and F. C.-H. Rhee, "Uncertain fuzzy self-organization based clustering: interval type-2 fuzzy approach to adaptive resonance theory," *Information Sciences*, vol. 424, pp. 69–90, 2018.

[37] C. Qiu, J. Xiao, L. Yu, L. Han, and M. N. Iqbal, "A modified interval type-2 fuzzy c-means algorithm with application in mr image segmentation," *Pattern Recognition Letters*, vol. 34, no. 12, pp. 1329–1338, 2013.

[38] Z. Ji, Y. Xia, Q. Sun, and G. Cao, "Interval-valued possibilistic fuzzy c-means clustering algorithm," *Fuzzy Sets and Systems*, vol. 253, pp. 138–156, 2014.

[39] C. Qiu, J. Xiao, L. Han, and M. N. Iqbal, "Enhanced interval type-2 fuzzy c-means algorithm with improved initial center," *Pattern Recognition Letters*, vol. 38, pp. 86–92, 2014.

[40] H. Tizhoosh., "Image thresholding using type-2 fuzzy sets." *Pattern Recognition*, vol. 38, pp. 2363–2372, 2005.

[41] S. Dhar and M. K. Kundu, "A novel method for image thresholding using interval type-2 fuzzy set and bat algorithm," *Applied Soft Computing*, vol. 63, pp. 154–166, 2018.

[42] M. E. Yüksel and M. Borlu, "Accurate segmentation of dermoscopic images by image thresholding based on type-2 fuzzy logic," *IEEE Transactions on Fuzzy Systems*, vol. 17, no. 4, pp. 976–982, 2009.

[43] M. Pagola, C. Molina, J. Fernandez, E. Barrenechea, and H. Bustince., "Intreval type-2 fuzy sets constructed from membership functions: Application to the fuzzy thresholding algorithm," *IEEE transactions on Fuzzy systems*, vol. 21, no. 2, pp. 230–244, 2013.

[44] C. Hwang and F. C.-H. Rhee, "Uncertain fuzzy clustering: Interval type-2 fuzzy approach to *c*-means," *IEEE Transactions on Fuzzy Systems*, vol. 15, no. 1, pp. 107–120, 2007.

[45] D. Wu and J. M. Mendel, "Uncertainty measures for interval type-2 fuzzy sets," *Information sciences*, vol. 177, no. 23, pp. 5378–5393, 2007.

[46] A. Blake and A. Zisserman, "Weak continuity constraints in computer vision," *Internal Report*, 1986.

[47] ——, *Visual Reconstruction*. Cambridge, MA, USA: MIT Press, 1987.

[48] J. M. Mendel and R. I. B. John., "Type-2 sets made simple." *IEEE Transactions on Fuzzy Systems.*, vol. 10, pp. 117–127., 2002.

[49] A. Blake and A. Zisserman, "Localising discontinuities using weak continuity constraints," *Pattern recognition letters*, vol. 6, no. 1, pp. 51–59, 1987.

[50] S. Aminifar and A. Marzuki, "Uncertainty in interval type-2 fuzzy systems," *Mathematical Problems in Engineering*, vol. 2013, 2013.

[51] M. Nie and W. W. Tan, "Towards an efficient type-reduction method for interval type-2 fuzzy logic systems," in *Fuzzy Systems, 2008. FUZZ-IEEE 2008.(IEEE World Congress on Computational Intelligence). IEEE International Conference on*. IEEE, 2008, pp. 1425–1432.

[52] J. Li, R. John, S. Coupland, and G. Kendall, "On nie-tan operator and type-reduction of interval type-2 fuzzy sets," *IEEE Transactions on Fuzzy Systems*, vol. 26, no. 2, pp. 1036–1039, 2018.

[53] M. Acharyya, R. K. De, and M. K. Kundu, "Extraction of features using m-band wavelet packet frame and their neuro-fuzzy evaluation for multitexture segmentation," *IEEE Transactions on Pattern Analysis and Machine Intelligence*, vol. 25, no. 12, pp. 1639–1644, 2003.

[54] M. K. Kundu and M. Acharyya, "M-band wavelets: Application to texture segmentation for real life image analysis," *International Journal of Wavelets, Multiresolution and Information Processing*, vol. 1, no. 01, pp. 115–149, 2003.

[55] C. Li, R. Huang, Z. Ding, J. C. Gatenby, D. N.Metaxas, and J. C. Gore., "A level set method for image segmentation in the presence of intensity inhomogeneitics with application to MRI." *IEEE Transactions on Image processing.*, vol. 20, no. 7, pp. 2007–2016, 2011.

[56] Y. J. Zhang, "A survey on evaluation methods for image segmentation," *Pattern recognition*, vol. 29, no. 8, pp. 1335–1346, 1996.

[57] G. L.-E. W. Yong, "Evaluation measures for segmentation," *matrix*, vol. 1, no. 1, p. 2.

[58] B. Ziółko, D. Emms, and M. Ziółko, "Fuzzy evaluations of image segmentations," *IEEE Transactions on Fuzzy Systems*, vol. 26, no. 4, pp. 1789–1799, 2018.

[59] Y. Zhang., "A survey on evaluation methods for image segmentation. image segmentation evaluation: A survey of unsupervised methods." *Pattern Recognition.*, vol. 29, pp. 1335–1346, 1996.
[60] R. Peng and P. Varshney, "On performance limit of image segmentation algorithms," *Computer Vision and Image understanding*, vol. 132, pp. 24–38, 2015.
[61] *https://data.broadinstitute.org/bbbc/BBBC029/*.
[62] *http://www.wisdom.weizmann.ac.il*.
[63] *https://www.eecs.berkeley.edu/Research/Projects/CS/vision/bsds/*.
[64] *http://mehmetsezgin.net*.
[65] *http://www.bic.mni.mcgill.ca/brainweb/*.
[66] *http://www.oasis-brains.org/*.
[67] A. Hoover, G. Jean-Baptiste, X. Jiang, P. J. Flynn, H. Bunke, D. B. Goldgof, K. Bowyer, D. W. Eggert, A. Fitzgibbon, and R. B. Fisher, "An experimental comparison of range image segmentation algorithms," *IEEE transactions on pattern analysis and machine intelligence*, vol. 18, no. 7, pp. 673–689, 1996.
[68] *http://data.broadinstitute.org/bbbc/BBBC038/*.

Soumyadip Dhar received his B.E and M.E degree from University of Burdwan and MAKAUT respectively. Currently he is pursuing Phd. from the university of Calcutta, India. He also holds the position of Assistant Professor in the department of IT of the RCC Institute of Information Technology, Kolkata,India. His current research interest includes Image/video processing& analysis, soft computing, computer vision, machine intelligence and data security. He has contributed several prestigious journals, international conferences and edited books.

Malay K. Kundu ($M'90 - SM'99$) received his B. Tech., M. Tech. and Ph.D (Tech.) degrees in Radio physics and Electronics all are from the University of Calcutta. In 1982, he joined the Indian Statistical Institute (ISI), Calcutta, as a faculty member. He is the Co-Principal Investigator of the Center for Soft Computing Research: A National Facility (established by Govt. of India). He superannuated from the service of the institute as Full Professor in December 2013 and subsequently became INAE distinguished chair professor in the Machine Intelligence Unit (MIU) of this Institute till 2016. Currently, he is a visiting professor at the MIU, ISI, Kolkata.

He is a Fellow of the International Association for Pattern Recognition, USA (FIAPR), Indian National Academy of Engineering (FNAE), National Academy of Sciences (FNASc.), India and the Institute of Electronics and Telecommunication Engineers (FIETE), India. A senior member of the IEEE, USA and the founding life member & was Vice President (2004-14) of the Indian Unit for Pattern Recognition and Artificial Intelligence (IUPRAI). He received the prestigious VASVIK award for industrial research in the field of Electronic Sciences & Technology for the year 1999. He also received in the year 1986, the Sir. J. C. Bose memorial award from the Institute of Electronics and Telecommunication Engineers (IETE), India.

His current research interest includes Digital image processing, Machine learning, Content Based Image Retrieval, Computational Intelligence, Wavelets, Video processing & analysis and Computer vision,. He has contributed 6 edited book volumes, about 150 research papers in well known and prestigious archival journals, international refereed conferences and in the edited monograph volumes. He is the holder of ten U.S patents, three International and two E.U patents